

Properties of the upper part of the last glacial loess-palaeosol sequence at Savudrija (Istria, Croatia) [Prezentacija]

Hećej, Nina

Supplement / Prilog

Permanent link / Trajna poveznica: <https://urn.nsk.hr/um:nbn:hr:169:594538>

Rights / Prava: [In copyright](#)/[Zaštićeno autorskim pravom.](#)

Download date / Datum preuzimanja: **2024-05-05**



Repository / Repozitorij:

[Faculty of Mining, Geology and Petroleum
Engineering Repository, University of Zagreb](#)



**6th Regional Scientific Meeting on
Quaternary Geology: Seas,
Lakes and Rivers
Ljubljana, Slovenia**

28th September 2021

**Properties of the upper part of the Last
Glacial loess-palaeosol sequence at Savudrija
(Istria, Croatia)**

NINA HEĆEJ & GORAN DURN



INTRODUCTION

- **Fieldwork**
- 7,5 m thick loess-palaeosol sequence in Savudrija, Istria (CRO)
- performed within NALPS (*engl. North Adriatic Loess-Paleosol Sequences*) project
- **Reason for the survey?**
- To investigate the **origin, age and features of the six horizons** (depth 0-205 cm) located in the upper part of the loess-palaeosol sequence from Istria, Croatia
- **How?**
- By applying detailed mineralogical, geochemical, pedophysical and micromorphological analyzes
- + OSL dating

GEOGRAPHICAL POSITION AND GEOLOGY OF THE RESEARCHED AREA

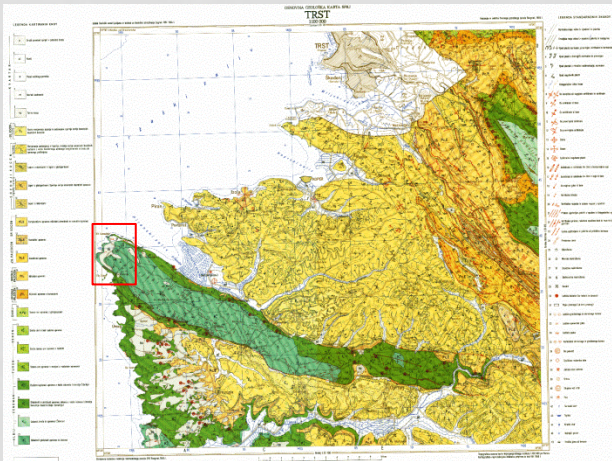


Figure 2. A crop of the Basig Geological Map of Republic of Croatia, 1:100000 Trst sheet

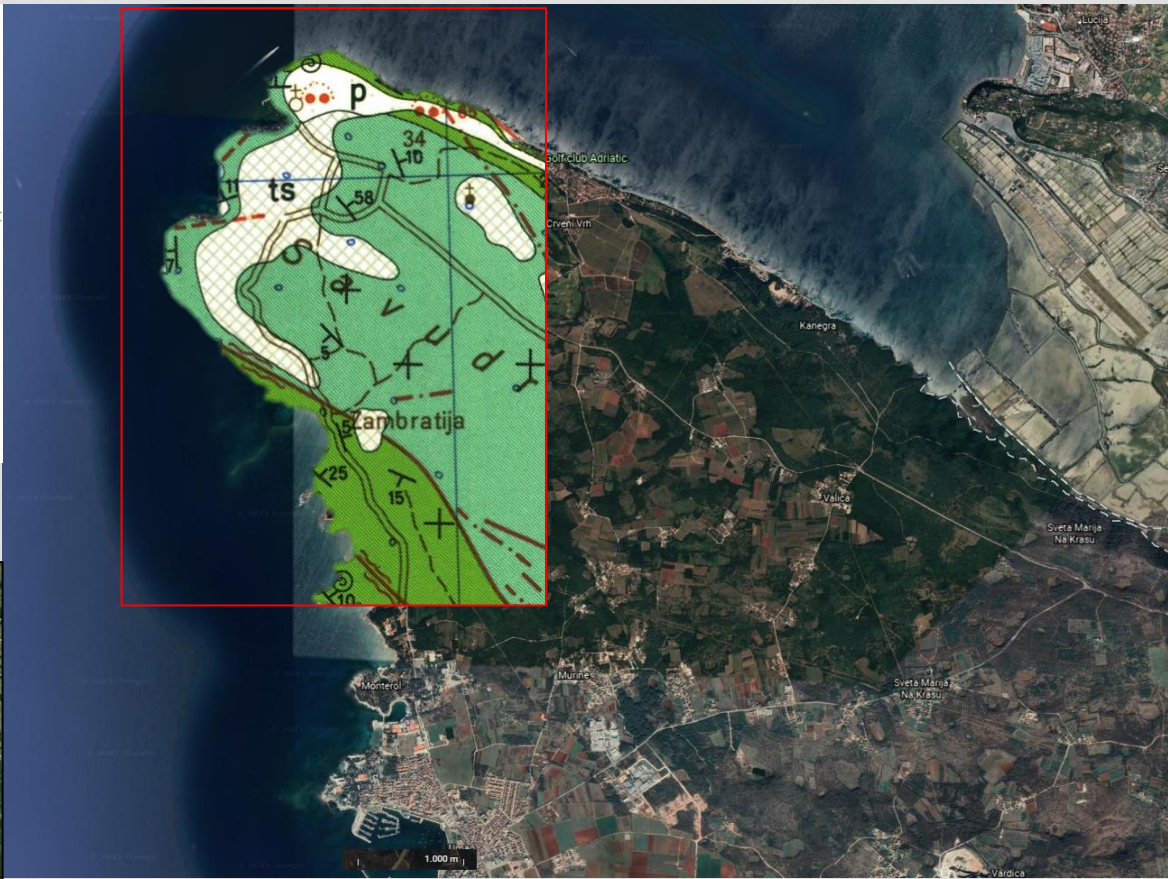
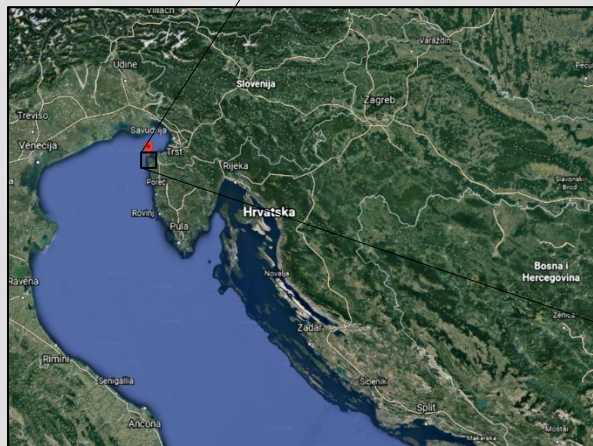


Figure 1. Geographical position of Savudrija profile (modified after https://earth.google.com/web/search/Savudrija/@45.01709433,14.29590456,5.54042896a,199229.65405215d,35y,-0h,0t,0r/data=CmJaOBIyCiUweDO3N2I3Yjk1YzczMmNkYTk6MHgyNjAwYWQ1MTUzMzZINzgyKglTYXZlZHJpamEYASABfYKJAluNcT3wlNIQBGIywFYPANFQBInNdNoQOVw4QCHMSaBxhegOQA?utm_source=earth7&utm_campaign=ign-vine&hl=hr)



Figure 3. a) Profile through pedosedimentary complex with shown sampling sites; b) the investigated part of the pedosedimentary complex

FIELDWORK RESULTS

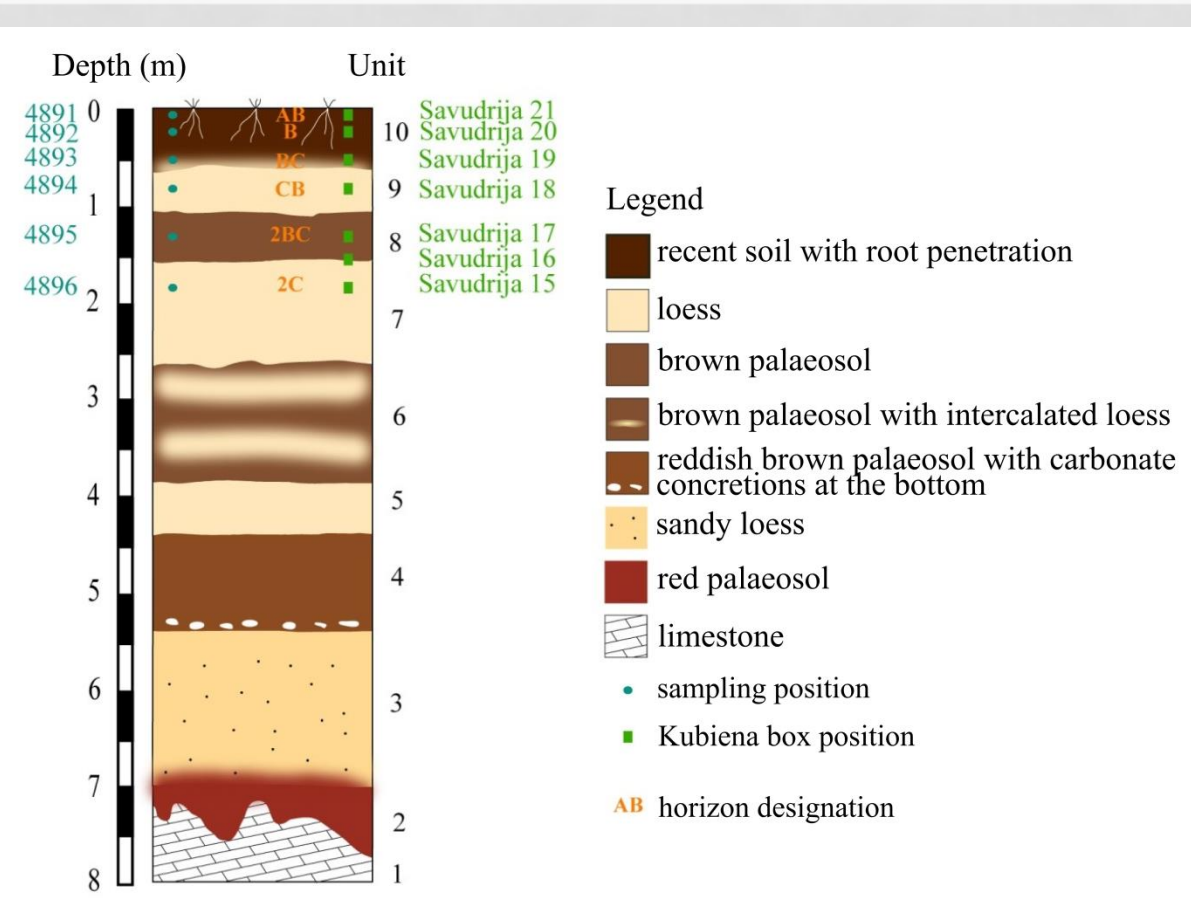


Figure 4. The graphical log of the Savudrija loess-palaeosol sequence with indicated sampling positions analyzed within this thesis (modified after ZHANG et al., 2018)

Munsell's color chart:

- 4891 : 7,5 YR 5/3 (brown)

Other samples's hues: 10 YR (light-brown to yellowish-brown)

- color: goethite

LABORATORY WORK

- detailed chemical analysis
- physical and chemical analysis of the paleosols (incl. CEC and base saturation, particle size analysis, analysis of iron and manganese oxides and hydroxides soluble in dithionite-citrate bicarbonate and oxalate)
- mineral composition analysis (XRD method)
- optically and infrared stimulated luminescence (OSL & IRSL)
- micromorphological analysis of thin sections.

Table 4. Chemical properties of the upper part of the Savudrija profile

Sample ID	Horizon	pH		Description	CaCO ₃ [%]	Description	Humus [%]	Description	Organski C (%humus/1,72) [%]	Total C[%]	Organic C (Total C - anorganic C) [%]
		H ₂ O	KCl								
4891	AB	8,22	7,38	alkaline	1,7	Low carbonate content	2,53	Low humosity	1,47	2,05	1,85
4892	B	8,87	7,30	alkaline	7,4	Low carbonate content	2,79	Low humosity	1,62	1,57	0,69
4893	BC	9,14	7,53	alkaline	24,8	Medium carbonate content	4,91	Medium humosity	2,85	3,85	0,87
4894	CB	9,20	7,58	alkaline	34,7	High carbonate content	2,77	Low humosity	1,61	5,24	1,08
4895	2BC	8,58	7,59	alkaline	27,5	High carbonate content	5,82	High humosity	3,38	4,37	1,06
4896	2C	8,39	7,65	alkaline	36,1	High carbonate content	2,40	Low humosity	1,40	5,54	1,20

CATION EXCHANGE CAPACITY (CEC) & PERCENT BASE SATURATION (BS)

Table 6. CEC values of the upper part of the Savudrija profile

CEC = b(Mg) + b(Na) + b(K) + b(Ca) [meq/100g]		
Sample	b(Mg) + b(Na) + b(K) + b(Ca)	RSD [%]
4891	79,954	0,8805
4892	87,661	1,0857
4893	107,811	1,3056
4894	138,861	1,1542
4895	147,626	1,7274
4896	142,318	1,3447

CEC

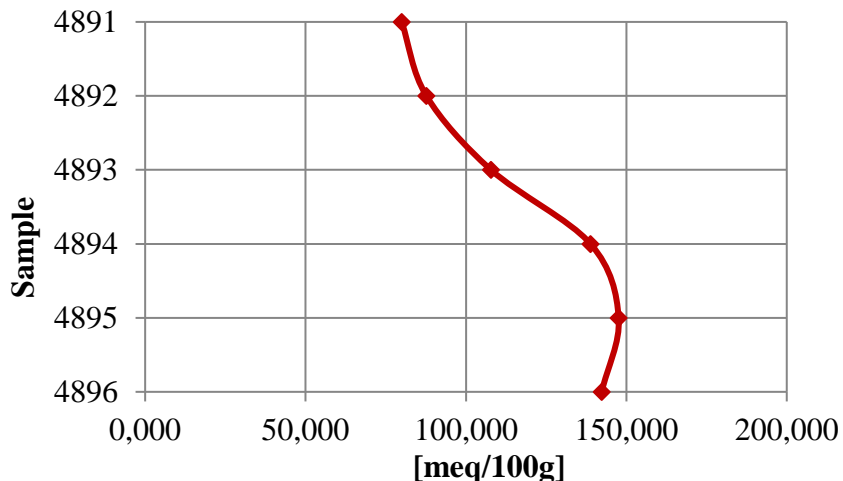


Figure 9. CEC values by profile depth

Base saturation - Mg

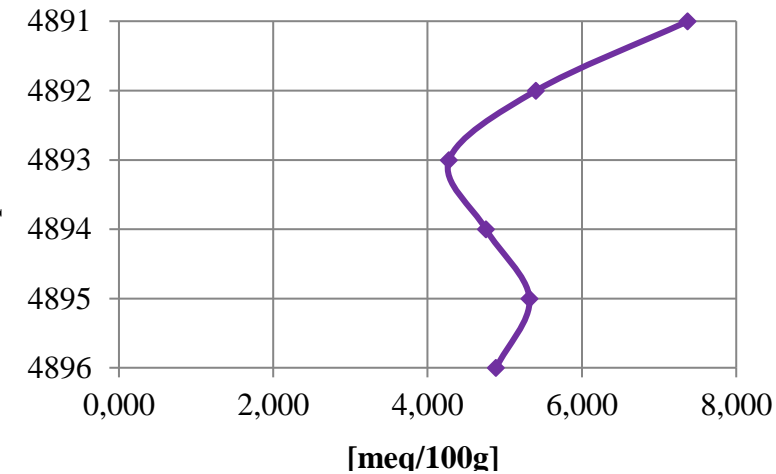


Figure 7. Percent base saturation of Mg^{2+}

Base saturation - Ca

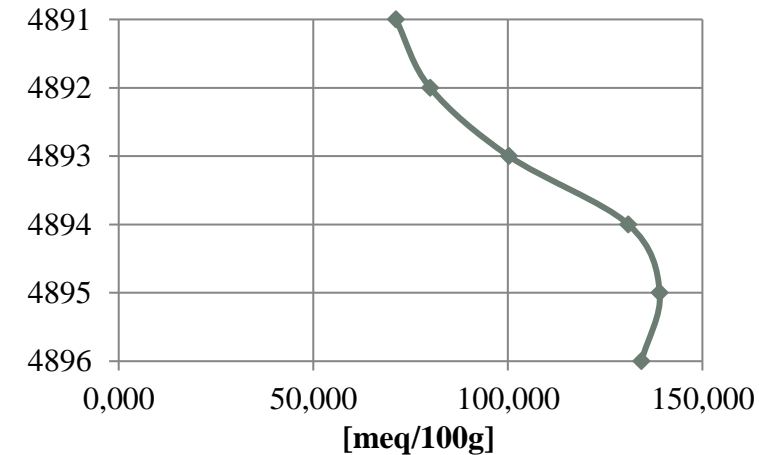
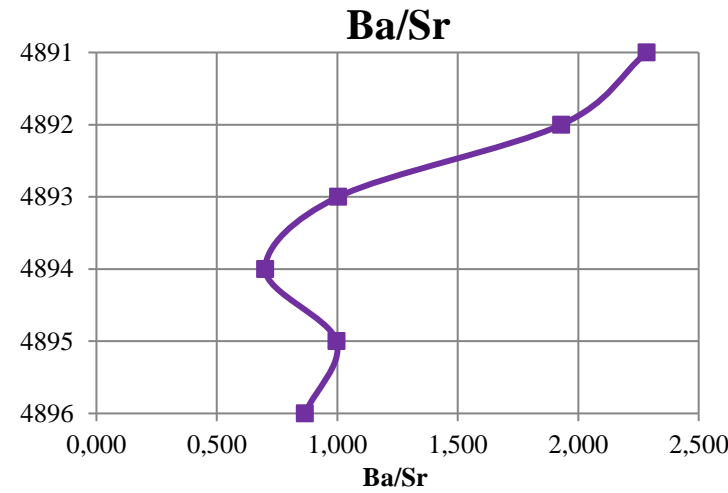
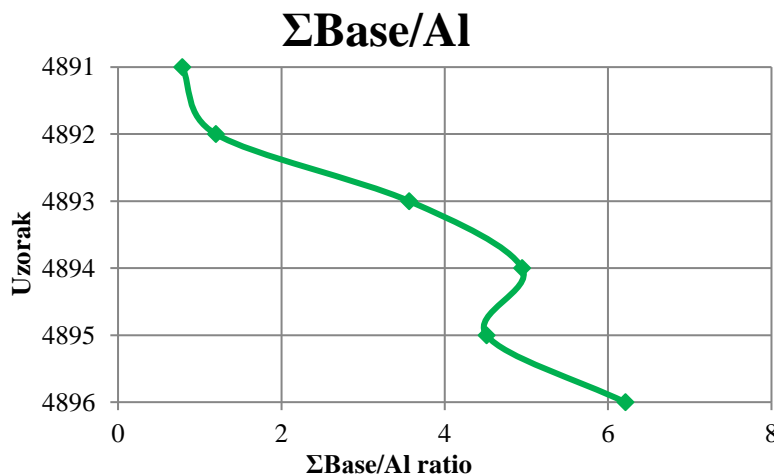
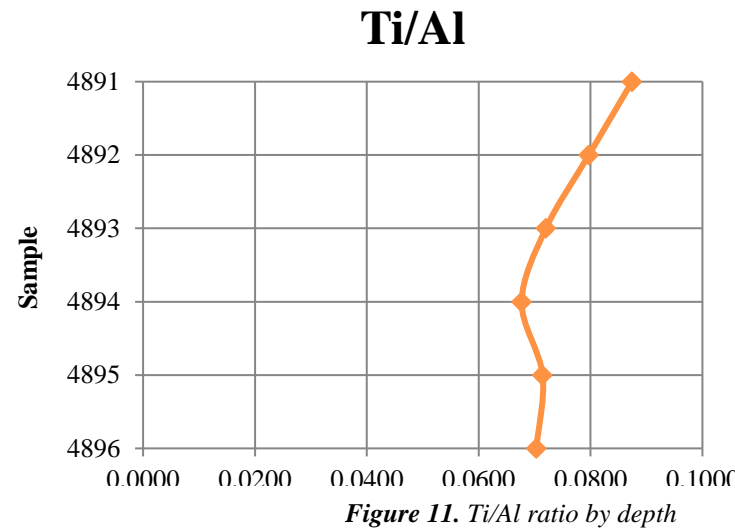
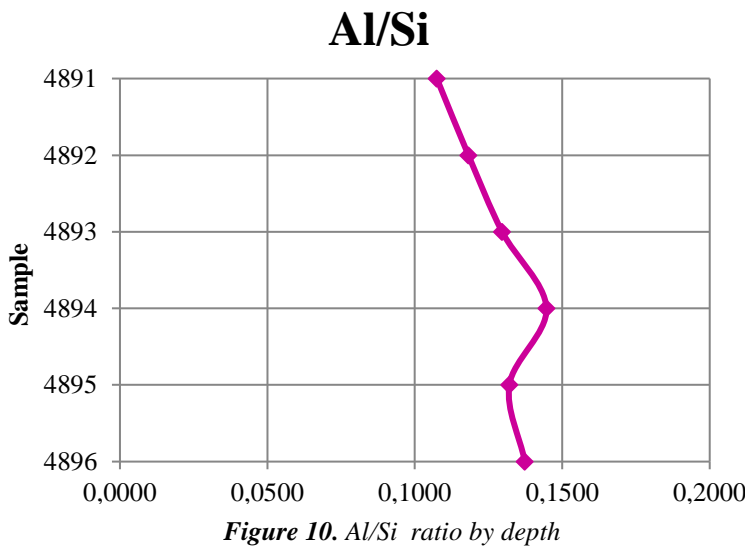


Figure 8. Percent base saturation of Ca^{2+}

GEOCHEMICAL RATIOS



DCB & OXALATE SOLUBLE IRON

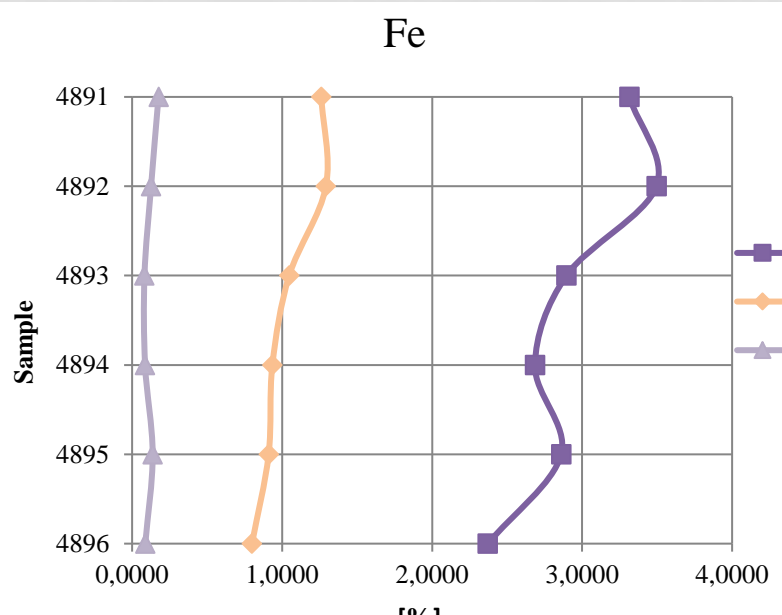


Figure 14. total (Fet), dithionite-soluble (Fed) and oxalate soluble ((Feo) iron per profile depth

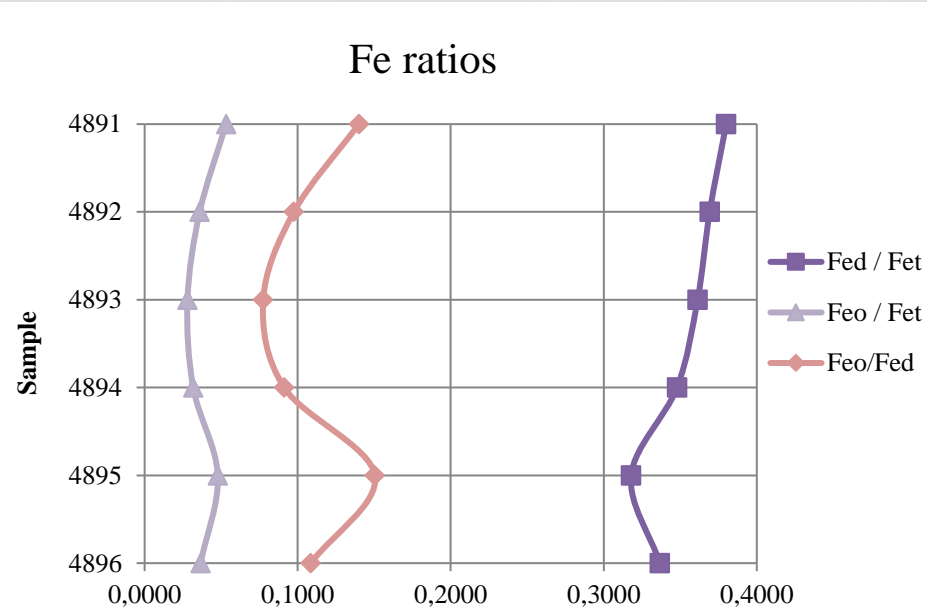


Figure 15. Ratios of total (Fet), dithionite-soluble (Fed) and oxalate soluble ((Feo) iron per profile depth

- The mean value of the $\text{Fe}_d / \text{Fe}_t$ ratio is 0.35, which according to ARDUINO et al. (1984) & DURN (1996), indicate a medium degree of weathering.

DCB & OXALATE SOLUBLE MANGANESE

- **Table 9.** Shares and ratios of total (Mn_t), dithionite-soluble (Mn_d) & oxalate soluble Mn (Mn_o).

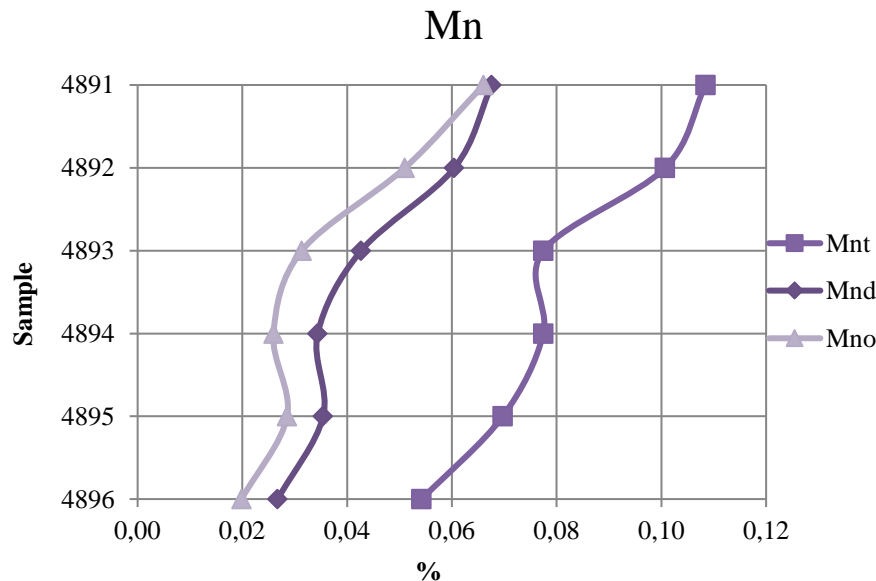


Figure 16. Total (Mnt), dithionite-soluble (Mnd) and oxalate (Mno) soluble manganese by profile depth

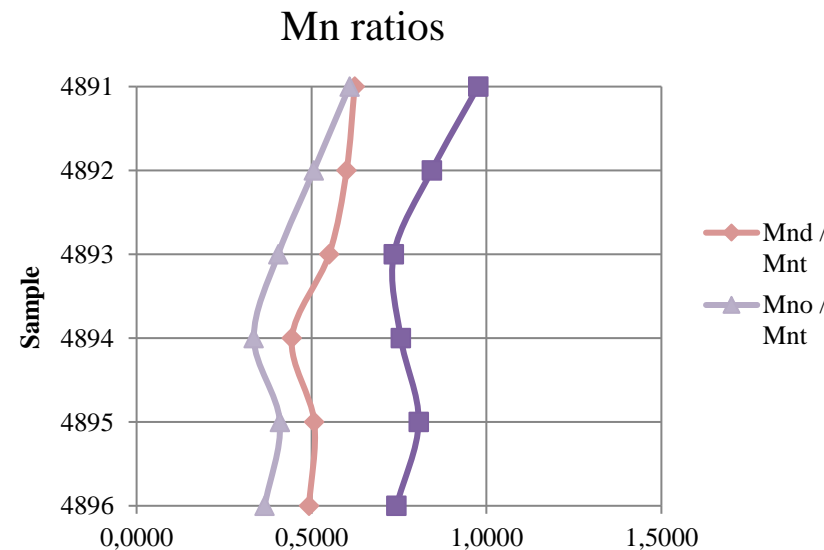


Figure 17. Ratios of total (Mnt), dithionite-soluble (Mnd) and oxalate soluble (Mno) manganese per profile depth

MODAL COMPOSITION

Table 12. Semiquantitative mineral composition of the clay fraction (particle size & $<2\mu\text{m}$) of samples after dissolution of carbonate (in wt %).

Sample	Clay component	Qtz	Pl	Kfs	Gt	Hm	Amph	Ill	Kln	Chl	14Å		Chl - Vrm	MM / NIM	AC
											S	Vrm			
4891 $<2\mu\text{m}$	25,90	6	+	?	+	-/?	?	++	+/++	++	++ (S i/ili Vrm)		+/++	+++	+
4892 $<2\mu\text{m}$	31,10	5	-	-	+	?	-	++	++	+/++	+/++	?	+/++	++/+++	+
4893 $<2\mu\text{m}$	26,30	5	-	-	+	?	-	++	++	+/++	++ (S i/ili Vrm)		+/++	++/+++	+
4894 $<2\mu\text{m}$	23,90	6	-	-	+	-	-	++	++	+/++	++ (S i/ili Vrm)		+/++	++/+++	+
4895 $<2\mu\text{m}$	21,40	7	-	-	+	-	-	++	++	++	? ++	? ?	++/+++	+/++	
4896 $<2\mu\text{m}$	20,60	5	-	-	+	-	-	++	++	+/++	? ?	? (Chl - Ill)	++/+++	+/++	

OSL & IRSL AGE

Table 13. OSL and IRSL ages of the upper part of the section

Sample ID	Lab ID	Depth [cm]	IRSL age [ka]	OSL age [ka]
SAV 7	4894	55 - 115	$17,5 \pm 1,2$	$8,9 \pm 0,6$
SAV 6	4896	165 - 205	$31,4 \pm 2,5$	$20,4 \pm 1,6$

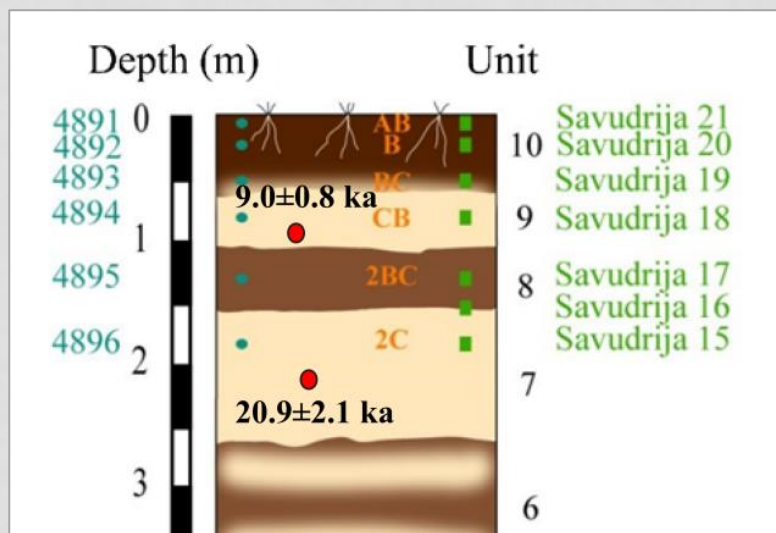


Figure 18. The graphical log of the upper part of Savudrija loess-palaeosol sequence OSL and IRSL ages of the two loess horizons (modified after ZHANG et al., 2018)

MICROMORPHOLOGICAL FEATURES

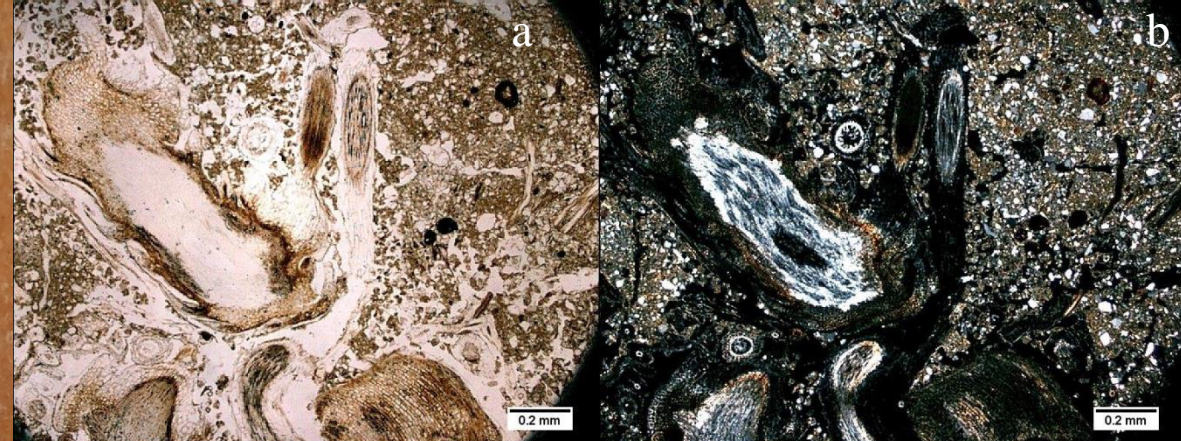
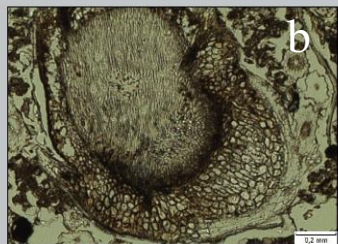
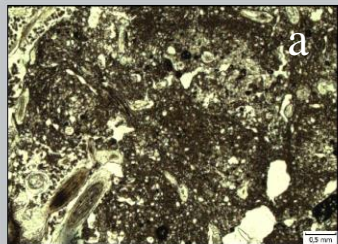


Figure 20. Savudrija 21: crystallisation of calcite in the internal part of the plant cell wall) a) PPL; b) XPL

Figure 19. Thin section Savudrija 21; a) c/f distribution in the thin section; pedofeatures: rhizoconcretions within voids and cracks, Fe/Mn oxide nodules , accumulation of dispersed organic matter(PPL); b) Rhizoconcretion (dimension 1,25 mm) with a pronounced honeycomb structure filled with secondary carbonate: b) (PPL); c) (XPL)

Geology: Seas, Lakes and Rivers
jubljana, Slovenia

MICROMORPHOLOGICAL FEATURES

Savudrija 20

- microstructure:** spongy/vesicular
- pedofeatures:** dominant rhizoliths, with Fe- & Mn nodules, few pedorelicts (brown coloured well-rounded forms)
- pedality:** weak, with predominantly angular grains and poor sorting

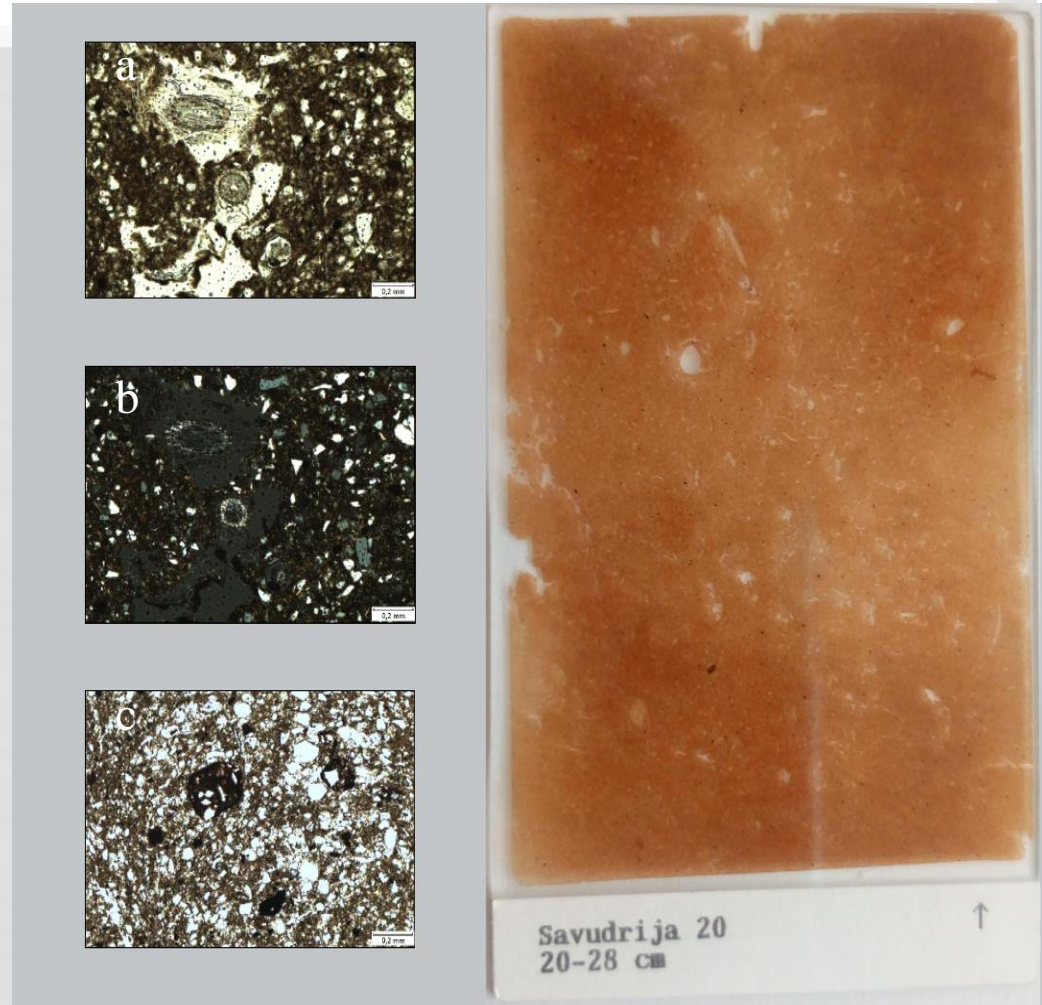


Figure 21. Savudrija 20; a) rhizoliths with secondary crystallised calcite within voids (PPL); b) rhizoliths with secondary crystallised calcite within voids (XPL); c) Fe-Mn nodules with embedded Qtz-grains (PPL)

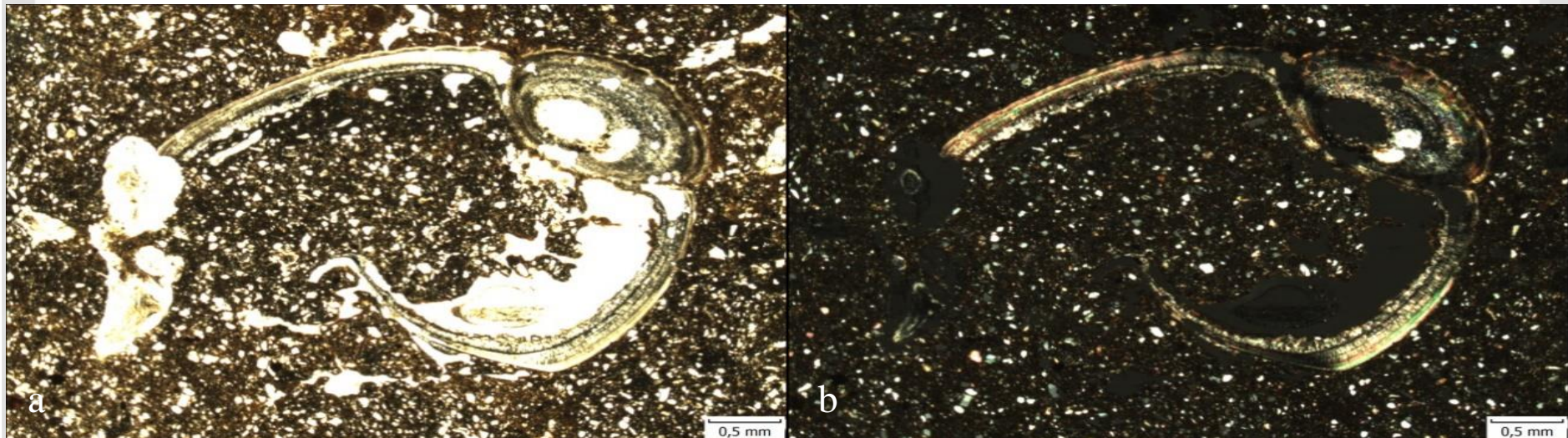


Figure 23 . Savudrija 19: axial cross section of the brachiopod shell (PPL & XPL)

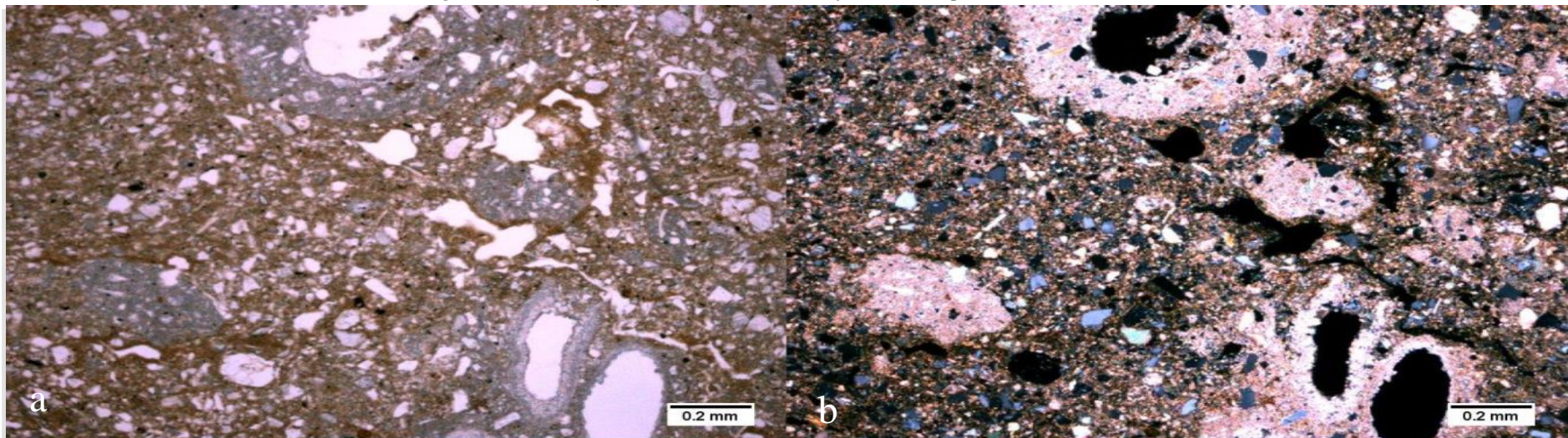
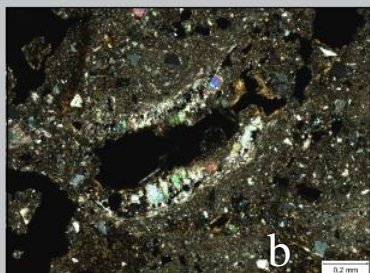
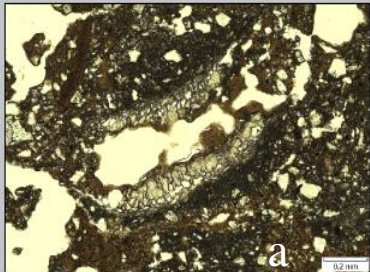


Figure 24. Accumulation of rhizoconcretions and chain aggregation of secondary carbonates along the edges of the cavities (PPL & XPL)

MICROMORPHOLOGICAL FEATURES



Savudrija 18

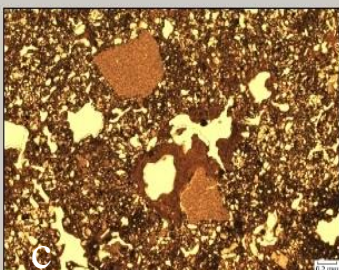
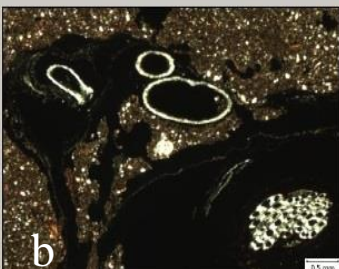
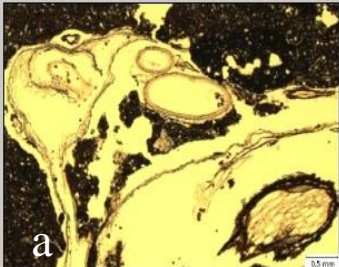
-**microstructure:** channely with *vughs*

- **pedofeatures:** clay coatings, Fe & Mn nodules, agglomeration of secondary crystalised calcite, higher amount of organic matter

-**pedality:** weak, with angular to rounded aggregates; in lower part of the section stronger bioturbation is observed

Figure 25. Thin section Savudrija 18; **a)** crystallized agglomerated grains of secondary calcite and clay coating along the edge of the crack (PPL), **b)** crystallized agglomerated grains of secondary calcite and clay coating along the edge of the crack (XPL), **c)** An elongated fragment of charcoal (PPL)

MICROMORPHOLOGICAL FEATURES



Savudrija 17

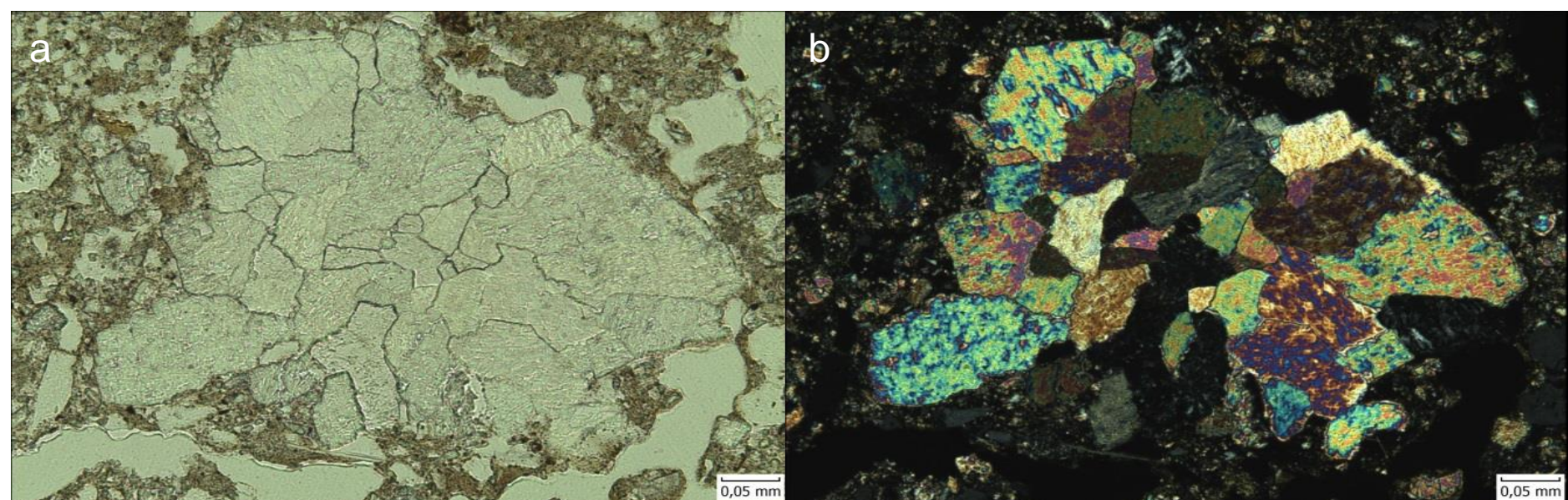
-**microstructure:** channelly to spongy

-**pedofeatures:** clay and calcite coatings, replacement of quartzite grain with calcite, abundance of Fe/Mn oxide noduls, rhizocretions

Higher amount of organic matter

-**pedality:** weak, with angular to rounded aggregates

Figure 26. accumulation of dispersed organic matter, christalization of secondary calcite along the mollusc shell fragments in thin section Savudrija 17
a) (PPL), b (XPL)



Slika 26. a) replacement of chert grain with calcite (PPL), b) replacement of chert grain with calcite(XPL) observed in thin section Savudrija 17

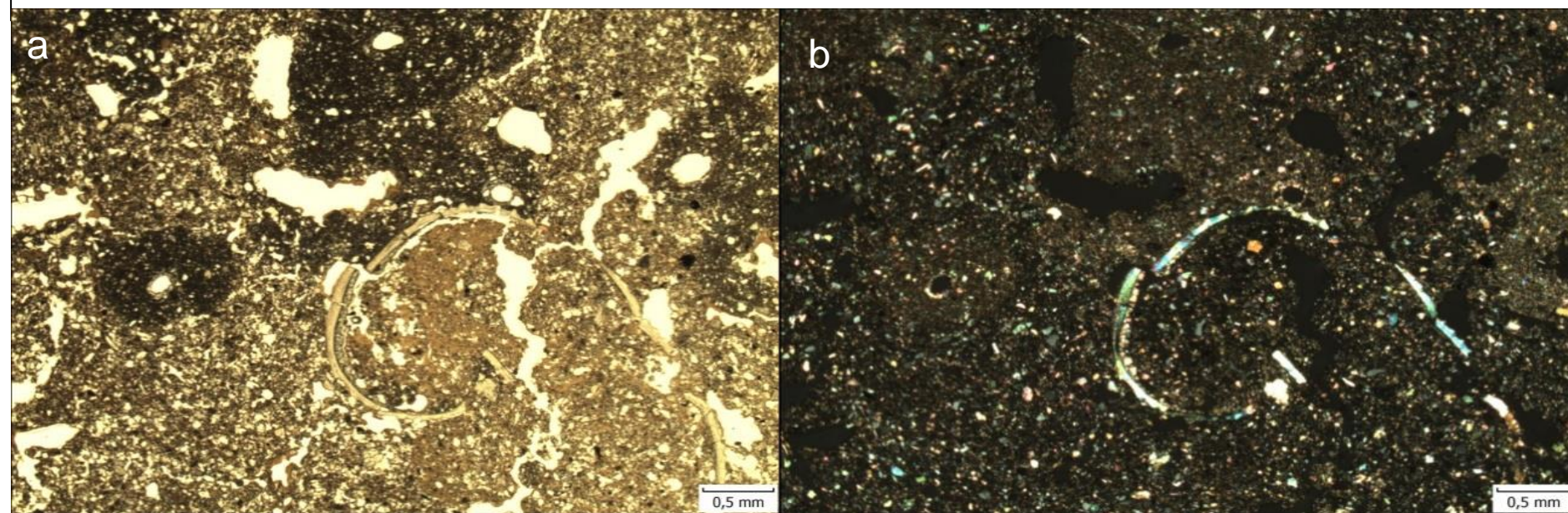
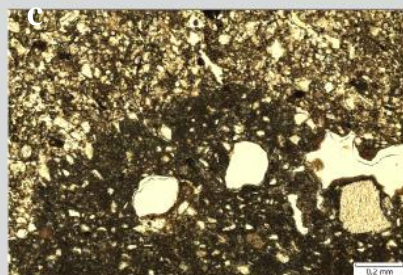
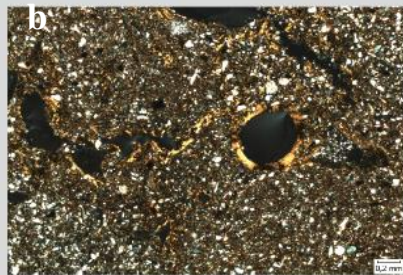
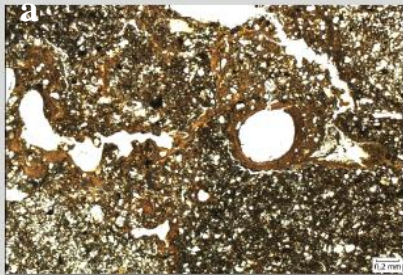


Figure 27. Pedofeatures observed in thin section Savudrija 17; a) Rhizoconcretions with observed crystallization of calcite along the cell wall (PPL), b) Rhizocretions with observed crystallization of calcite along the cell wall (XPL)

MICROMORPHOLOGICAL FEATURES



Savudrija 16
150-158 cm

Savudrija 16

-**microstructure:** spongy with vughs and channels

-**pedofeatures:** clay coatings, Fe/Mn oxide nodules and secondary crystalized calcite

- replacement of chert grain with calcite; molluscs shell fragments observed

-high amount of organic matter

-**pedality:** weak to medium

Figure 28. Savudrija 16; **a)** dispersed organic matter and clay coatings along the edge of cracks and cavities (PPL), **b)** (XPL), **c)** Dispersed organic matter in contact with the grain of chert (PPL),

MICROMORPHOLOGICAL FEATURES

Savudrija 15

- microstructure:** spongy to vuggy-channelly
- **pedofeatures :** Fe-Mn oxide nodules, a lot of clay coatings; agglomerated grains of sekundary crystalized calcite
- pedality:** weak to medium

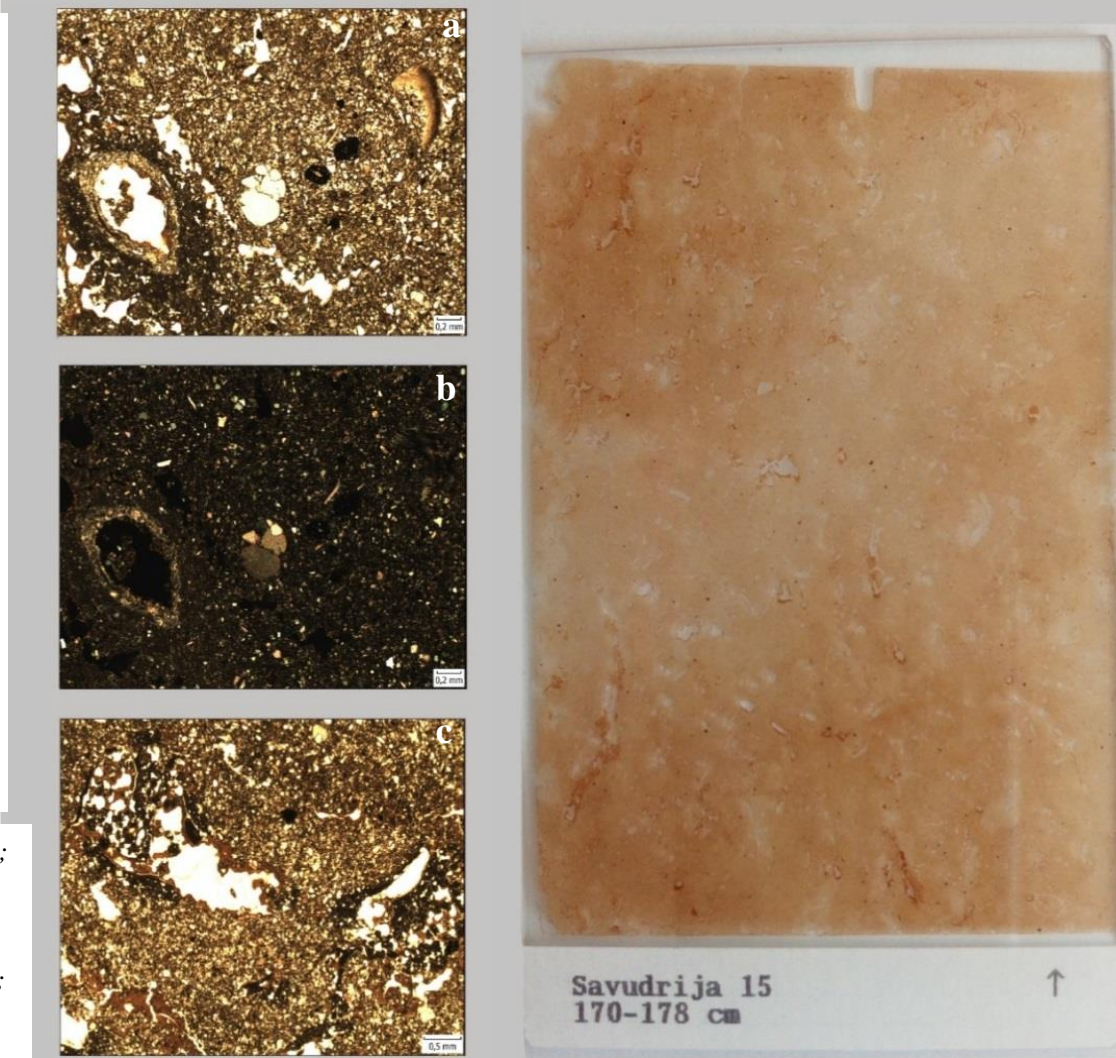


Figure 29. Pedofeatures observed in thin section Savudrija 15;
a) dispersed organic matter, accumulation of clay coatings along the edge of the channel and vughs, rounded dark brown to black Fe - Mn nodules, nodules of agglomerated calcite and secondary crystallized calcite within the shell fragments (PPL);
b) (XPL); c) dispersed organic matter and clay coatings along the edge of vughs (PPL)

CONCLUSION

- The uppermost part of the sequence studied was represented by presumably polygenetic soil developed on loess (AB-B-BC-CB) underlain by brown palaeosol developed on older loess (2BC-2C). Based on the Sm/Nd and La/Ce geochemical ratios (SHELDON & TABOR, 2009), it was also determined that the loess parent material examined in this study has the same provenance as the materials examined in BANIČEK (2016) and DURN et al. (2018a, b).
- XRD analysis revealed that all soil samples contain a significant amount of quartz, plagioclase, alkali feldspar, illitic material, kaolinite, chlorite, 14 Å minerals (vermiculite and/or smectite), mostly irregular mixed-layer clay minerals, goethite and amorphous components, whose content increases with depth.
- Based on quartz OSL dating, the age of the studied soil horizon CB is 9 ± 0.8 ka and of soil horizon 2C is 20.9 ± 2.1 ka (ZHANG et al., 2018).
- Micromorphological studies of the uppermost part of the section revealed two superimposed loess substrates in which (palaeo)sols developed. significant share of rhizoconcretions, ferrous/manganese oxide nodules and clay coatings, which indicate that there have been a significant illuviation in the horizons of the uppermost part of the Savudrija pedosediment complex.



Thank you :)

As part of the research preparation, this work has been supported in part by the Croatian Science Foundation under the projects ACCENT (3274) and WIANLab (8054)